INSTITUTE FOR HIGH ENERGY PHYSICS

IHEP 93-117

V.F.Konstantinov, R.N.Krasnokutsky, R.S.Shuvalov,
A.A.Solodkov, E.A.Starchenko, V.V.Sushkov, A.M.Zaitsev,
R.I.Dzhelyadin, S.V.Kopikov, O.V.Solovyanov

BEAM TESTS OF "SPACAL" TYPE MODULES FOR A HIGH PRESSURE GAS CALORIMETER

Protvino 1993

Abstract

Konstantinov V.F., Krasnokutsky R.N., Shuvalov R.S. et al.: Beam Tests of "Spacal" Type Modules for a High Pressure Gas Calorimeter: IHEP Preprint 93-117. – Protvino, 1993. – p. 19, figs. 10, refs. 24

High pressure gas modules with cylindrical ionization chambers for a Very Forward Calorimeter (VFC) were constructed and tested in the IHEP U-70 electron beam. The amplifiers were used in a remote mode (3m long cables). The module performance at small angles was tested in the energy range of $10 \div 30$ GeV using different gas mixtures like $Ar + CH_4$, $Ar + CF_4$ and pure CF_4 at the pressure of $20 \div 40$ Atm. The best value of $\sigma(E)/E$ reached is 18% at the angle 5.7° for 30 GeV electrons. The design was found to be adequate for future use in ATLAS/LHC.

Аннотация

Константинов В.Ф., Краснокутский Р.Н., Шувалов Р.С. и др. Тесты модулей газового калориметра высокого давления: Препринт ИФВЭ 93-117. – Протвино, 1993. – 19 с., 10 рис., библиогр.: 24.

Созданы и испытаны на пучке электронов с энергией $10 \div 30$ GeV на ускорителе ИФВЭ У-70 модули ионизационного газового калориметра высокого давления с электродами имеющими аксиальную симметрию. Усилители подсоединялись к прибору кабелями длиной 3 м. Исследовались характеристики модулей под малыми углами налетающего электрона с использованием газовых смесей типа $Ar + CH_4$, $Ar + CF_4$ и чистого CF_4 при давлении $20 \div 40$ Атм. Наилучшее энергетическое разрешение $\sigma(E)/E = 18\%$ достигнуто при угле 5.7° для электронов с энергией 30 GeV. Предложенная конструкция отвечает требованиям предъявляемым к переднему калориметру установки ATLAS/LHC.

INTRODUCTION

The main purpose of a forward calorimeter is to contribute to the measurement of missing P_t by covering high $\mid \eta \mid$ regions and tagging very forward jets. This determines the goals for forward calorimeter performance in future SuperColliders. They are $\mid \eta \mid$ coverage of $(3 \div 4.5)$, measuring the smallest possible P_t, more or less modest energy resolution (at a level $100\%/\sqrt{E} \oplus 7\%$) and granularity, excellent time response ($\leq 25ns$) and the ability to operate after being exposed to a huge radiation dose of up to 1 MGy/year [1].

Baseline designs of the forward calorimeters for future collider devices usually cover $\mid \eta \mid = 3 \div 5$ at a distance of 5 - 20 meters from the bunch crossing point. Their depth is no less than 10λ and the number of readout channels per side is about 1000. The main goals of the designs are the following (see, e.g. [2-4]):

- transverse momentum sum measurement to select events with high missing P_t;
- transverse momentum sum measurement to reconstruct events with significant missing P_t (like $Higgs \rightarrow \tau\tau$, e.g.);
- jet determination; e.g., select events with heavy Higgs production through virtual W or Z exchange in the reaction $pp \rightarrow jet + jet + Higgs$;
- hermeticity of the whole device (E_{tot}, E_t conservation);
- reliability.

Most of these demands are satisfied with ionization pressurized gas calorimeters. Such detectors and their usefulness for future hadron colliders have been widely discussed during last years [5-16].

In this paper we give results on electron beam tests for pre-prototype modules of a Very Forward Calorimeter (VFC) for the LHC device ATLAS. High

pressure gas ionization tubes in "SPACAL like" geometry were chosen as an active media for the calorimeter,because they are relatively simple and reliable devices.

1. MODULES DESCRIPTION

Fig.1 shows the schematic views of a module . The module consists of a uniformly positioned set of $8 \times 8 = 64$ thin wall stainless steel tubes with their axis parallel to the beam direction. Two modules of slightly different sizes were completed, a "fine" and a "coarse" one. The inner diameter of the tubes is 7 mm, the outer one is 8 mm, their centers are 9.5 (12.0) mm apart . The edges of the tubes are welded to two gas collector plates. The space between tubes is filled with lead. The lead volume of the module has dimensions of $80 \times 80 \times 400 mm^3$ ($100 \times 100 \times 700 mm^3$). The final module length will have to be of the order of 2000 mm. The anodes are stainless steel rods with a diameter of 4.0 (3.0) mm and are kept in place with spacers. All that results in a gas gap between the anode and cathode of no more than 1.5 (2.0) mm.

All the anodes are multiplexed in fours within the gas collector volume and connected to the outside with special connectors capable to hold the high pressure and high voltage required. The impedance of each channel equals $8.5(12.5)\Omega$. Such a scheme gives 16 channels or elementary cells per module with a cross section of $19 \times 19 mm^2$ ($24 \times 24 mm^2$).

In average the radiation and interaction lengths for both modules are equal: $X_0 \approx 1.1 cm$ and $\lambda \approx 23. cm$.

Close to a module there is a box containing resistors, blocking capacitors and connectors forming the inner circuits of the channels. Gas mixture inlet and outlet go through the box and add to the module length no more than 150 mm.

The volume of the gas per module does not exceed 1/4th of the total one. Gas mixture of argon and some amount of other gases like methane (CH_4) or freon-14 (CF_4) at 20 - 40 Atm pressure were used as an active media.

This type of construction has the following advantages:

- excellent electrodynamical properties of the coaxial tubes (i.e. no signal dispersion, cross-talks, etc), which enables us to work with short signals;
- it is safer to have many small volumes under high pressure than a bigger one;
- it is easy to design, handle and repair a modular device; broken modules can be replaced.

2. ELECTRONICS

Each signal channel consists of a 3 m long connecting cable (we used four 50Ω impedance cables connected in parallel to have 12.5Ω), an amplifier, a 75 m long 50Ω cable to the control room, and an ADC. The ADC has a sensitivity of 0.25 pC/digit and a 12 bit range. During the run different gate widths were tested and a 20 ns gate was chosen. All the amplifiers were calibrated simultaneously between accelerator spills by feeding small signals from a row of calibrated capacitors into their inputs. The test signal responses as well as the ADC pedestals were recorded on the DST and used for calibration and correction off-line.

The amplifier circuit diagram is shown in Fig.2. The input transistor is used in Common-Base (CB) configuration without feed-back. Such a scheme was chosen because:

- neither CB nor Common-Emitter (CE) schemes with feed-back give good coupling to a low impedance cable (in our case it is $8 \div 12\Omega$); the chosen circuit is best matched.
- the nonlinearity of the head stage can be partly compensated by the nonlinearity of the output stage, if it has an opposite sign.
- the resulting small nonlinearity gives a small contribution to the overall measurement error but simplifies the scheme significantly.

The main features of the amplifier used are:

- adjustable input impedance of 12.5Ω; adjustment is done with the supply current of the head transistor (resistor R1),
- semigaussian shape of pulse response with 10 ns base-to-base time duration and without any afteroscillations,
- amplitude conversion of $\sim 1\mu V/e$ for δ-shape signal,
- current gain of ~ 1000,
- integral nonlinearity of $\sim 0.6\%$ for an output signal equal to 20 mA,
- equivalent noise charge (ENC FWHM) of $\sim 20 \cdot 10^3 e$ with a 3 m long cable at the input of the amplifier.

The noise level for the cable coupling between the detector and amplifier has been analyzed in detail in Refs. [17-21].

Here we should remark that at LHC energies the gain might be reduced significantly (because of higher energy deposition) and the last stage of the amplifier might be replaced with a linear summator (in the case of all elementary cells of a module being multiplexed together).

3. SET-UP

The calorimeter modules were tested with electron beams of 10, 20 and 30 GeV at the IHEP U-70 accelerator. Electrons were produced on an inner target and separated from hadrons and muons with Cherenkov counters.

The calculated value of $\Delta P/P \leq 1\%$; the contamination of the beam with hadrons, muons and wrong energy electrons was no more than 10%. The beam position was known with an accuracy of better than $\sigma \simeq 0.6mm$ on the face of the calorimeter.

The response of the devices was studied in dependence on high voltage, gas mixture and pressure, beam impact position X,Y and angle α, ADC gate delay and duration, etc.

4. TIME RESPONCE. SIGNAL DEPENDENCE ON HV

A calorimeter channel electrically acts like a bunch of four coaxial lines that are connected to an amplifier with a cable having nearly the same impedance. The amplifier response time to a δ-shape signal is of no more than 10 ns. Therefore, the output signal length is determined by the electron drift time within the gas gap of no more than 1.5(2.0)mm.

Three different gas mixtures were used during the tests: $Ar + x\%CH_4$, $Ar + x\%CF_4$ and pure CF_4. Each of them has some special features useful for calorimetry in general and for very forward calorimetry in particular [22-24].

The first mixture generally can improve electron-to-hadron (e/h) ratio due to the presence of hydrogen in the gas (the so called compensation effect). A rather significant CH_4 concentration is needed while the radiation hardness of methane as a media is questionable. Moreover, the drift velocity is not as high as desired.

The second one has a higher electron drift velocity (up to $12cm/\mu sec$) but needs a stronger electrical field.

And the last one, pure CF_4 has, in principle, an additional advantage of higher density, hence a better signal-to-noise ratio.

Fig.3a shows the signal shape for the mixture $Ar + 20\%CH_4$ at 40 Atm and an electrical field of 840 V/1.5mm. The duration of the signal agrees with the predictions, it is 25 ns base-to-base. The signal afteroscillation might be explained by a bad detector to cable impedance matching (8.5Ω to 12.5Ω) and rather high inductance of the electrical connection. Remember that the ADC gate width was 20 ns.

Fig.3b shows the signal shape for $Ar + 10\%CF_4$ at 20 Atm and the voltage of 1600 V/1.5mm (drift velocity $\sim 12cm/\mu s$). The duration of the signal base-to-base is less than 20 ns, which agrees with the calculations. For a real module 160-200 cm long the signal width may increase up to 25 ns according to longitudinal shower development, but this is still within LHC bunch crossing times.

A signal magnitude depending on applied voltage for $Ar + 20\%CH_4$ at 40 Atm is shown in Fig.4a. At 1300 V a maximum is reached that corresponds to the maximum drift velocity. The line in the picture is a simple polynominal fit. The collected charge agrees with the calculated value within 15%.

Fig.4b shows the dependence of the signal amplitude on the applied voltage for pure CF_4 at the pressure of 20 Atm. An asymptotic behaviour of the dependence is clearly visible and the maximum is twice as high as for the $Ar + 10\%CF_4$ mixture under the same conditions and is almost equal to the amplitude for $Ar + 20\%CH_4$ at 40 Atm (previous picture).

5. "GEOMETRY" EFFECTS

It is expected that the energy deposition in a calorimeter cell may depend on the electron entry point that is seen in Fig.5. The data shown was obtained with the "fine" structure device. The input particle positions are plotted for events depositing energy above a chosen threshold. Four patterns corresponding to different input angles of the electron are shown.

The pulseheight distribution for the area consisting of two by two elementary calorimeter cells ($38 \times 38mm^2$) is given in Fig.6(a). Fig.6(b) gives the average pulseheight in the same area measured in small pixels of the area (each of the four cells was partitioned into 10×10 pixels). The r.m.s. of the last distribution is clearly connected with the geometric characteristics of the device and we will call it "Geometry Inhomogeneity Factor" (GIF) from now on.

The GIF gives the main contribution to the energy resolution constant term and that is why we consider it so important.

Fig.6(c-h) shows average pulseheights as well as their r.m.s. over the pixels as a function of X for slices in Y. Zero means the center of the 2×2 cell region. The angle of the incident electron is $\alpha = 3.6^0$. Irregularities in the distributions are clearly visible and match the structure of the calorimeter cells.

For the "coarse" structure calorimeter the corresponding distributions are shown in Fig.7(a-h). The comparison between these two devices shows that rather small differences in "roughness" give a significant change in the geometrical factor and energy resolution values.

Here we have to mention that at small angles (up to 6^0) and energies below 30 GeV the effect of the geometrical factor on the resolution is small as compared to sampling fluctuations. Fig.8(a,b) illustrate this statement by giving the energy resolution as well as the GIF in dependence on the beam entry angle for both types of structure. The energy resolution for the "fine" structure calorimeter varies from 25% at the angle of 0.7^0 ($\mid \eta \mid = 5.0$) to less than 18% at the angle of 5.7^0 ($\mid \eta \mid = 3.0$). The resolution for the "coarse" one is much worse.

The influence of the geometry factor can be reduced by installing a converter far enough in front of the calorimeter to spread the shower particles over a wide enough area. As a test we placed converters of 1 to 4 $X_0 \approx 20cm$ in front of the calorimeter module. The results are shown in Fig.9(a,b).

The GIF drops almost linearly with the converter thickness for both structures. For a converter of $4X_0$ the GIF reduces by 40%. It follows that the same reduction can be expected for the constant term. For small thickness the total energy resolution improves with the converter thickness, so does the GIF. However, for the "fine" structure it begins to rise again for thick converters ($4X_0$). Probably it happens either due to energy loss fluctuations in a thick converter or shower energy leakage. In both cases the stochastic term increases.

All this supports that the geometric factor is only a small contribution to the energy resolution at input electron energies below 30 GeV.

The performance of the calorimeter for high energy hadrons and jets might be better. The showers in such a case have bigger transverse dimensions, wider spread and more numerous electromagnetic debris which makes the GIF decrease.

6. ENERGY DEPENDENCE OF THE RESOLUTION

Fig.10(a,b,c). shows the energy resolution and GIF values for the "fine" structure calorimeter measured at 10, 20 and 30 GeV beam energy for angles of $0.7^0, 2.2^0, 3.6^0$. It is rather evident that there is a very small energy dependence of the GIF.

The curves in the pictures represent the fit to the data with a dependence like:

$$\frac{\sigma(E)}{E} = \frac{A}{\sqrt{E}} \oplus B \oplus \frac{C}{E}.$$

C was determined as a value corresponding to the noise level of the calorimeter and is equal to 1.0 GeV for $Ar + 10\%CF_4$ at 30 Atm pressure. Both the

stochastic and constant terms decrease with the beam angle and for $\alpha = 3.6^0$ are: A=0.49, B=0.19.

CONCLUSION

The tested modules of a "SPACAL" type pressurized gas calorimeter have shown good performance in an electron beam at low energies and the "fine" structure module can be used as a pre-prototype for a forward calorimeter. A calorimeter made of such modules would have all the properties required for the usage in the future LHC detector ATLAS:

- short signals ($\leq 25ns$) matching LHC bunch crossing time,
- good enough energy and spatial resolution,
- simple and reliable construction which does not require high technology and can easily be mass-produced,
- radiation hardness depending only on the properties of such parts as spacers, blocking capacitors, cables etc.,
- modular structure allowing of convenient service and safe operation,
- having no internal amplification it has "self calibration properties" (electrical calibration).

Acknowledgments

We would like to thank all the members of the VErtex Spectrometer (VES) team for their efforts, without which this paper would have been impossible. One of us (E.A.S.) especially thanks Iris Abt from MPI for the help in preparing the text.

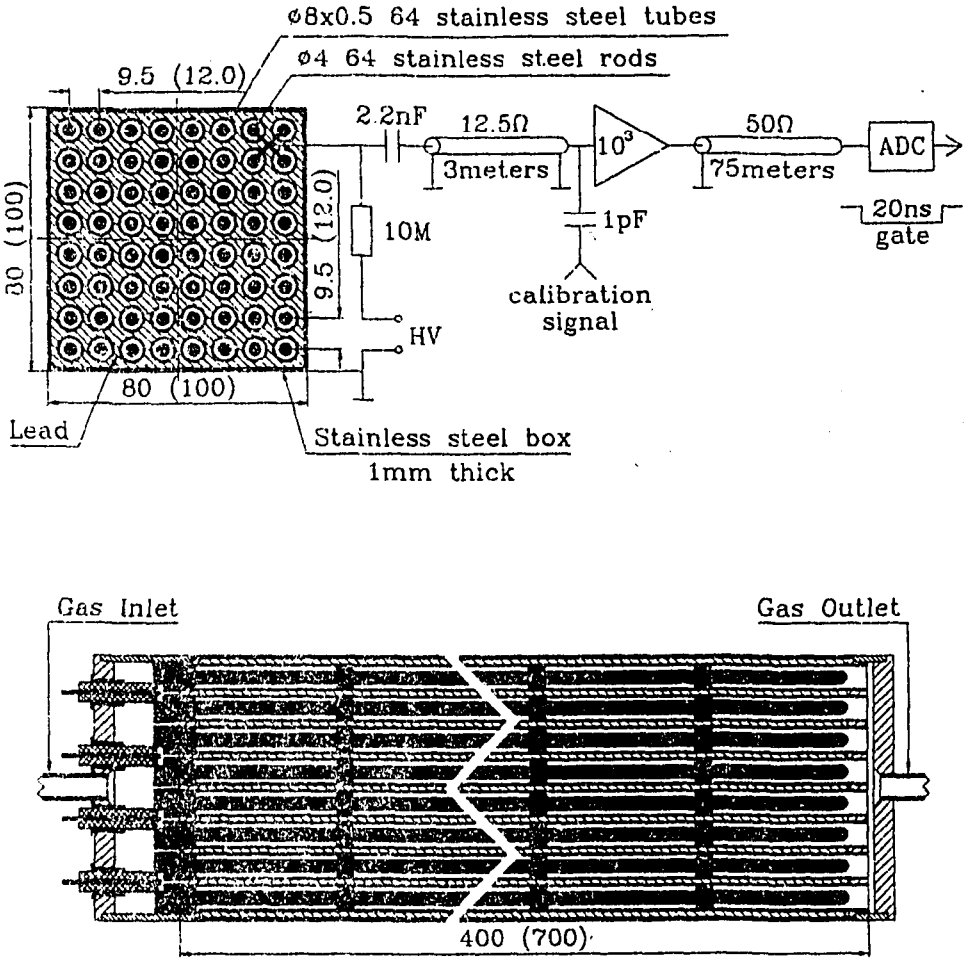

Figure 1. Schematic module view. The sizes are given for a "fine" structure and for a "coarse" one (in brackets).

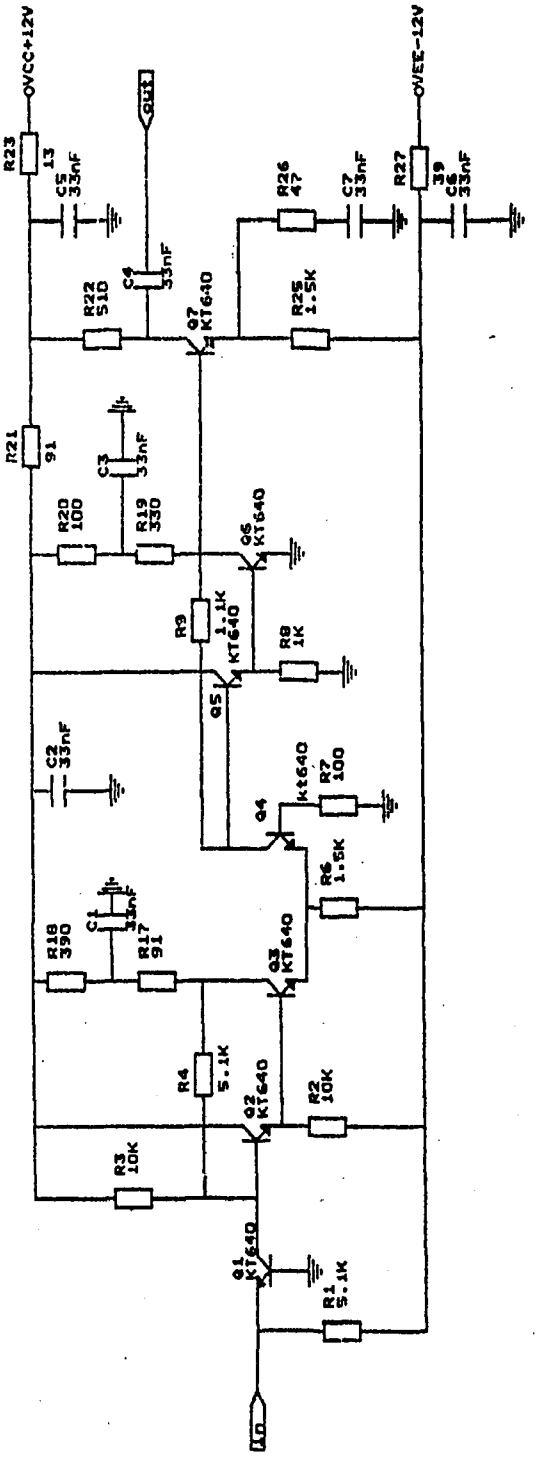

Figure 2. Curcuit diagram of the amplifier.

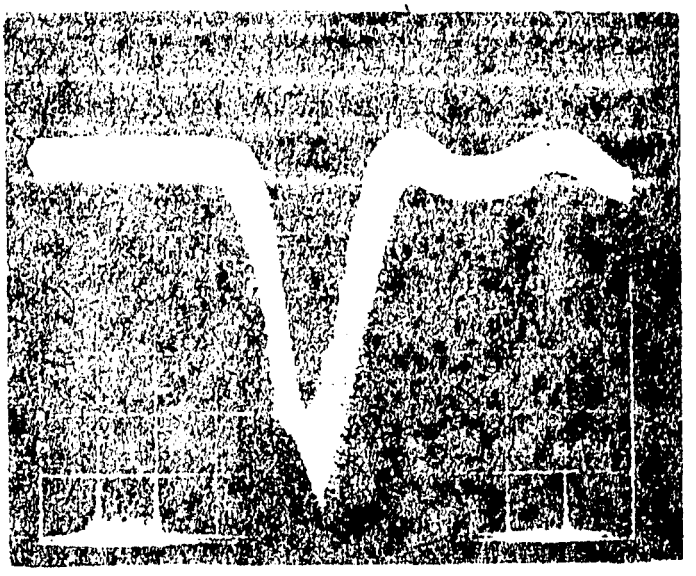

a) $Ar + 20\%CH_4$ 40Atm 840V/1.5mm

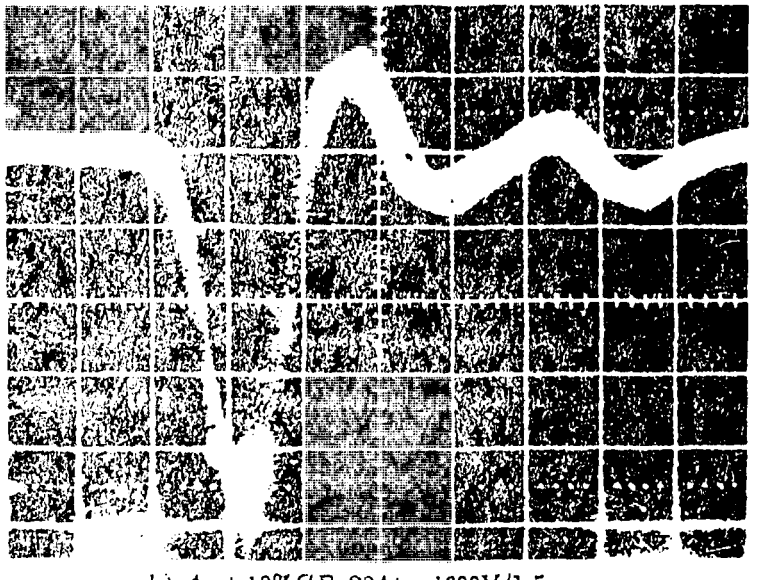

b) $Ar + 10\%CF_4$ 20Atm 1600V/1.5mm

Figure 3. Signal shape after an amplifier. *H.U.*=10 ns/div, *V.U.*=0.05 V/div.

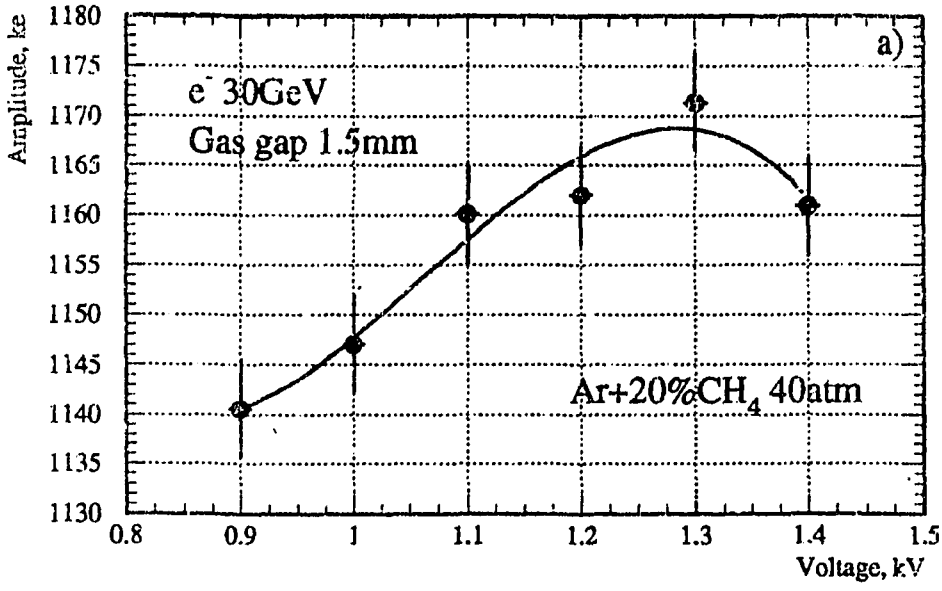

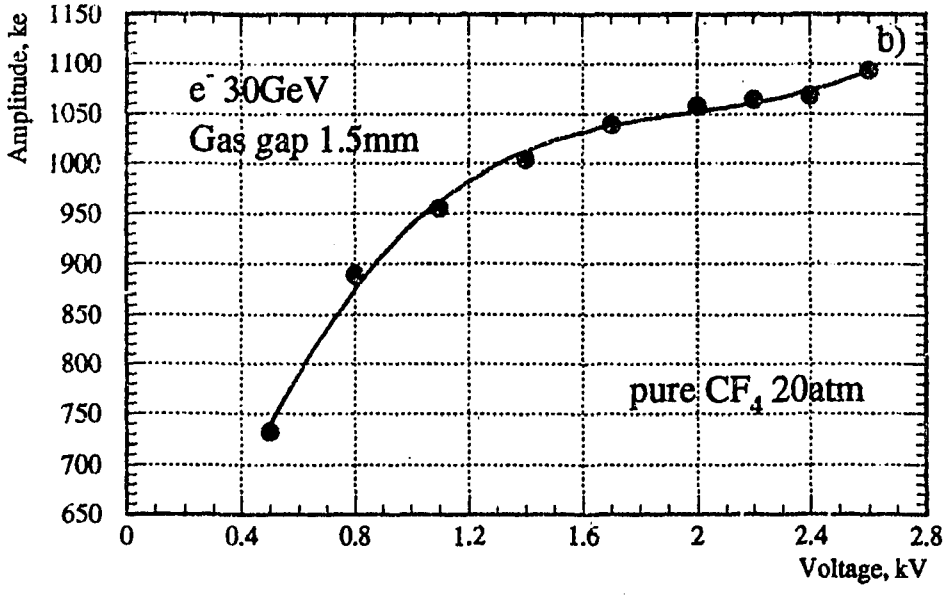

Figure 4. Signal amplitude vs applied voltage for $Ar + 20\%\ CH_4$ mixture and pure CF_4.

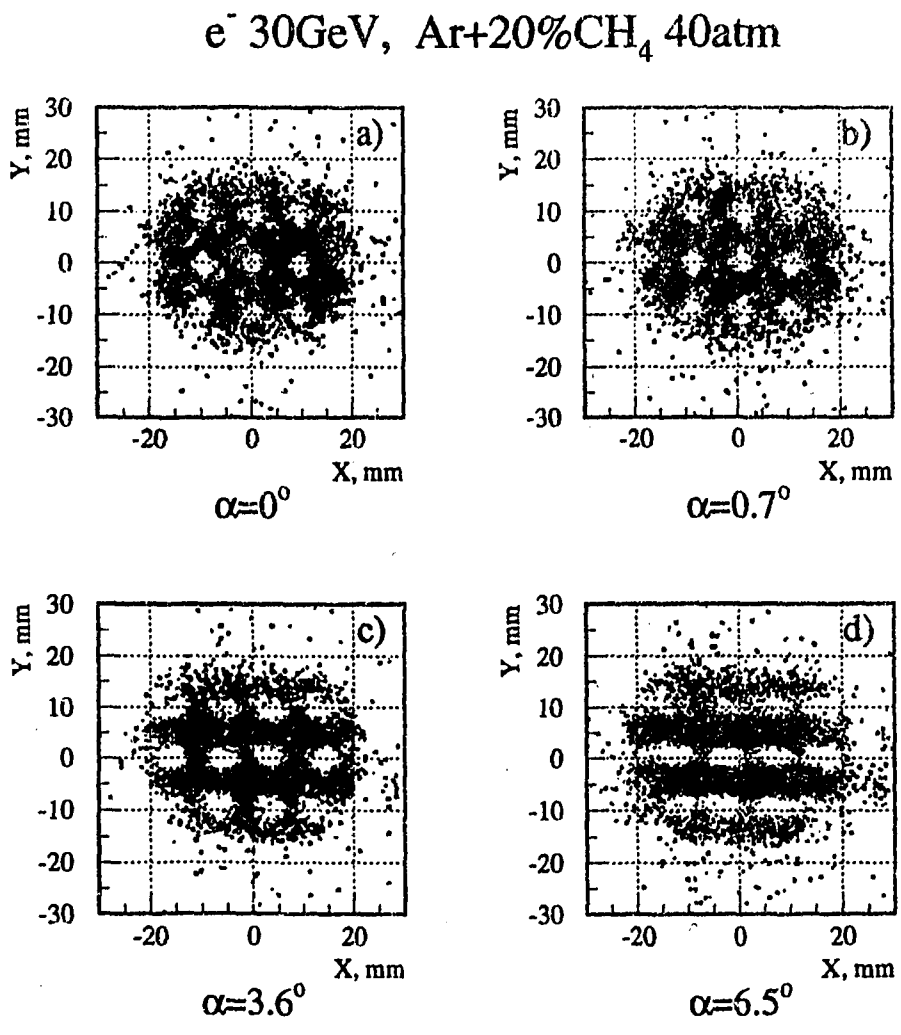

Figure 5. Transverse inhomogeneity of the "fine" module structure for different beam entry angles.

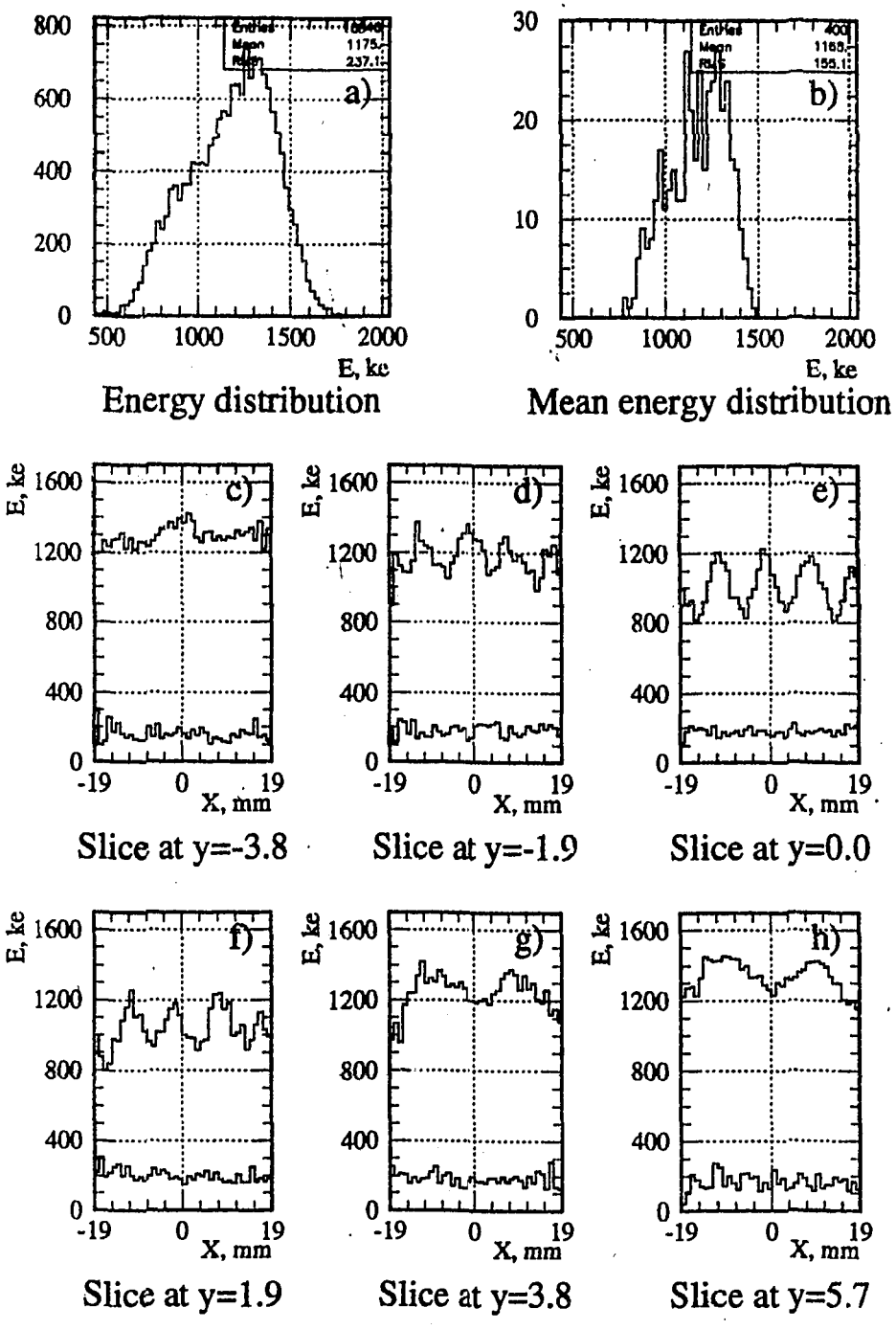

Figure 6. Deposited energy and geometrical inhomogeneity over a "fine" structure calorimeter cell.

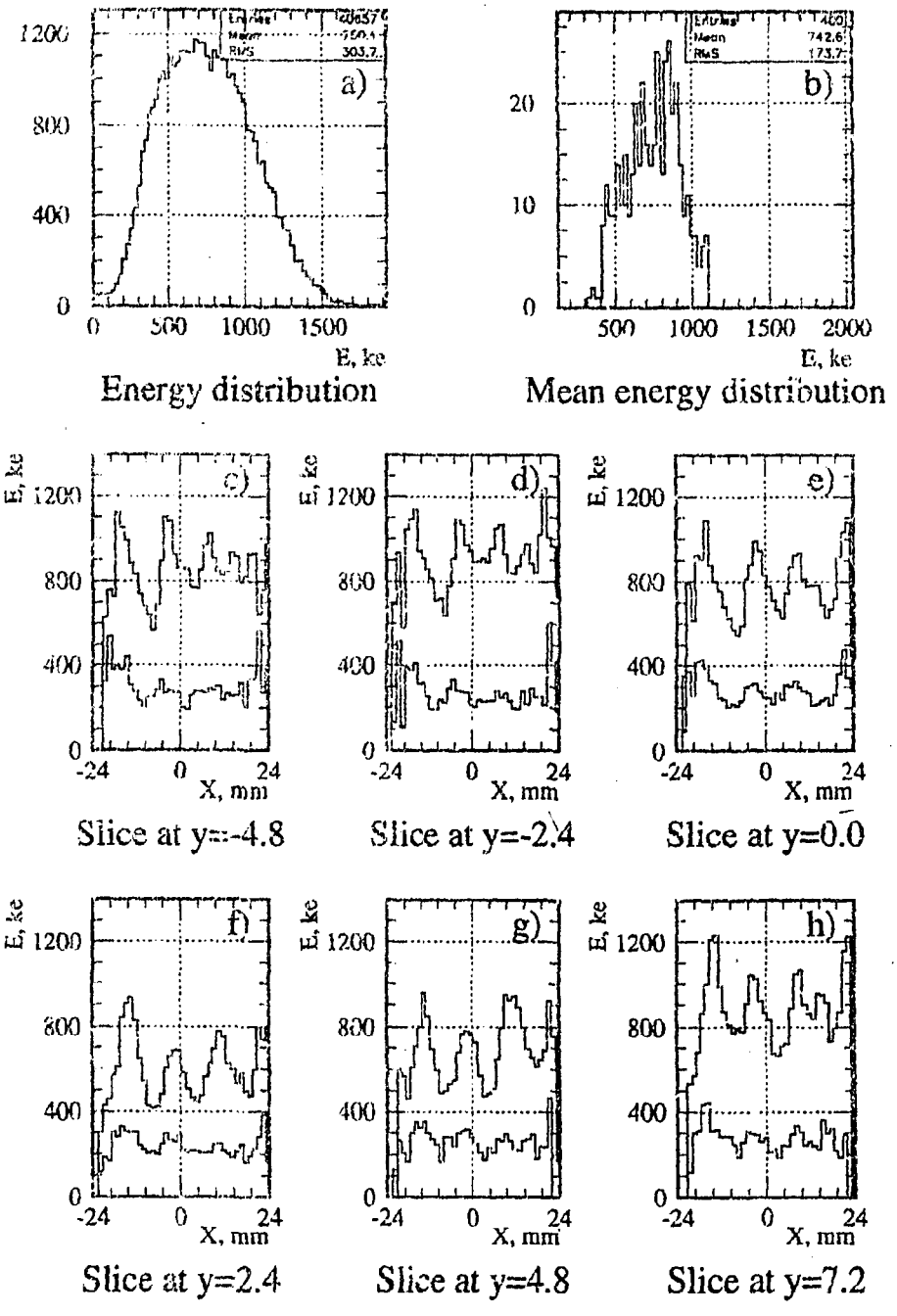

Figure 7. Deposited energy and geometrical inhomogeneity over a "coarse" structure calorimeter cell.

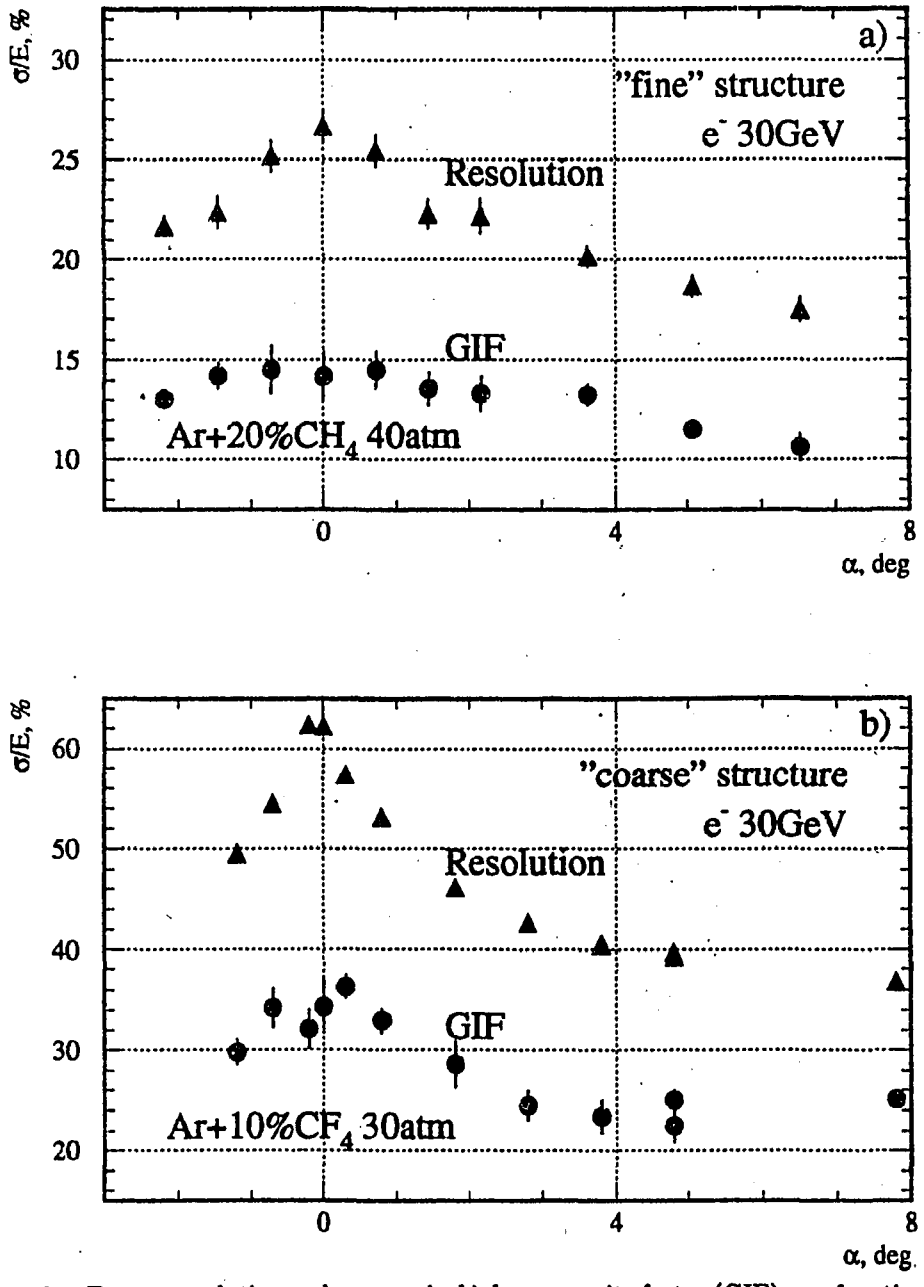

Figure 8. Energy resolution and geometrical inhomogeneity factor (GIF) as a function of beam input angle.

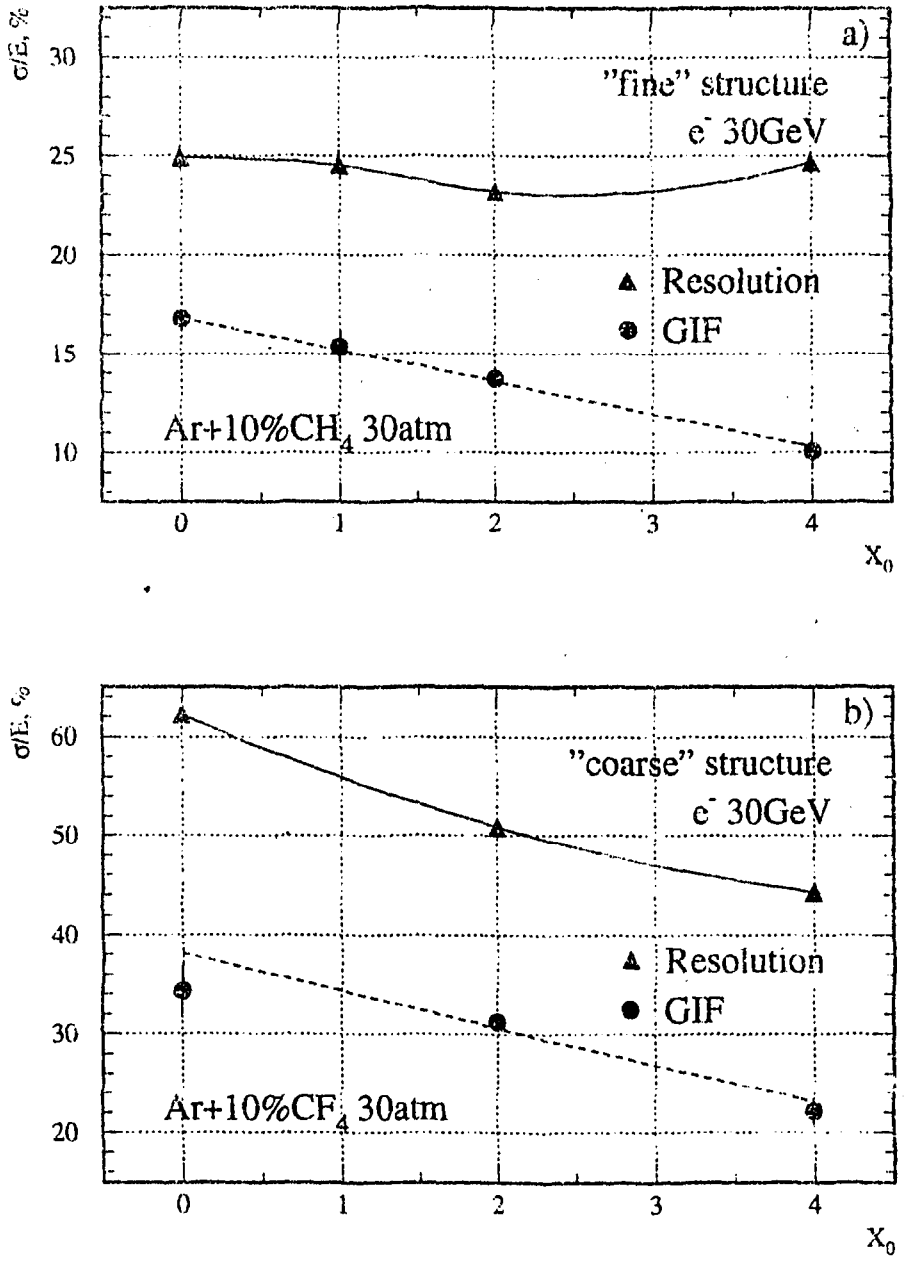

Figure 9. Energy resolution and geometrical inhomogeneity factor (*GIF*) as a function of a converter thinckness.

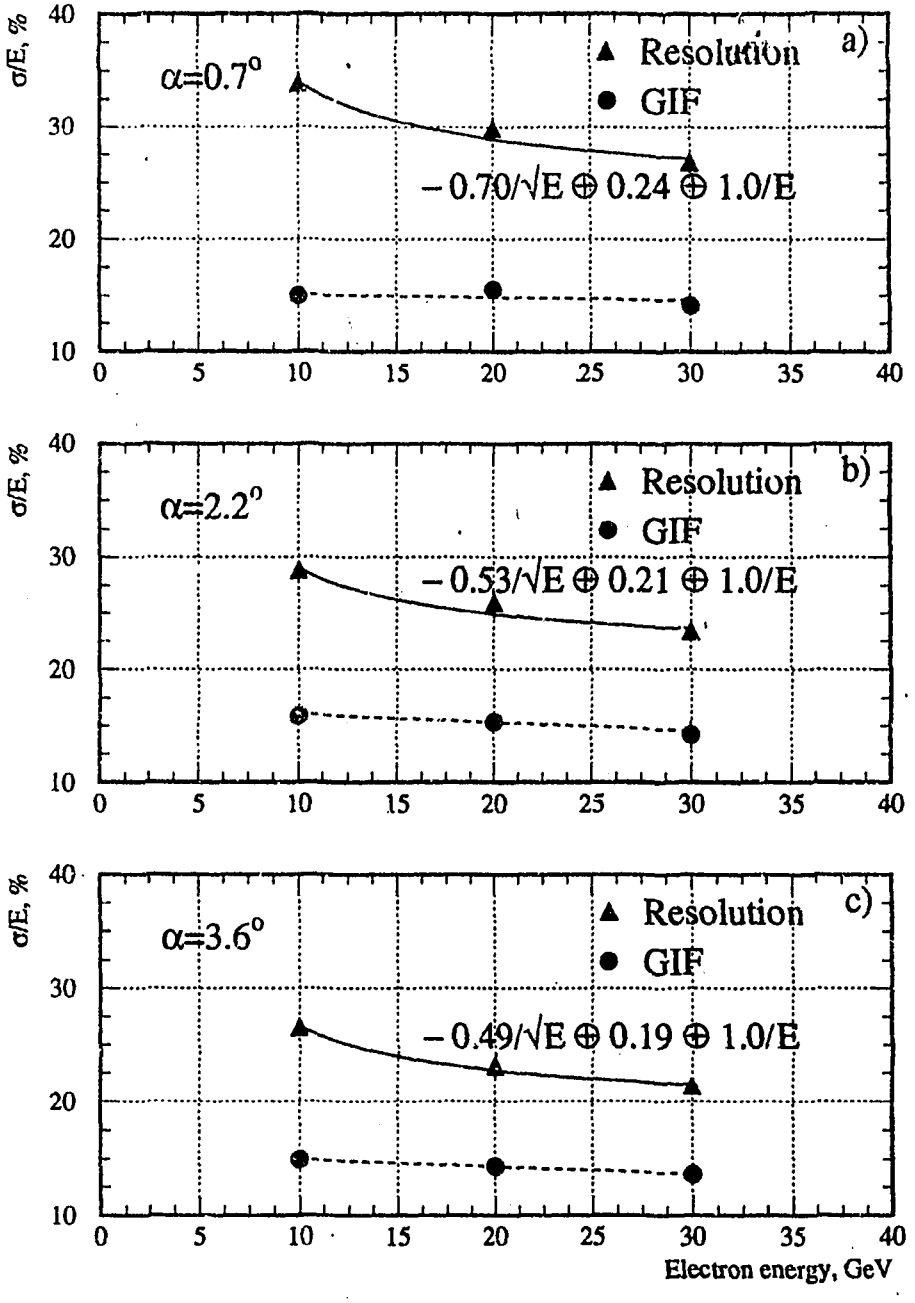

Figure 10. Energy resolution and geometrical inhomogeneity factor (GIF) for three beam input angles.

References

[1] Letter of Intent for a General-Purpose pp Experiment at the Large Hardron Collider at CERN. CERN/LHCC/92-4, LHCC/I 2, 1 October 1992.

[2] Moers T. et al.. Large Hardron Collider Workshop , Aachen, 4-9 October 1990, Proceedings, CERN 90-10, v.2, p.418.

[3] Seymour M.H. Large Hardron Collider Workshop , Aachen, 4-9 October 1990, Proceedings, CERN 90-10, v.2, p.557.

[4] Zmushko V.V. Preprint IHEP 91-176, Protvino, 1991.

[5] Baskakov V.I. et al. Nucl.Instr. and Meth. 159(1979) 83.

[6] Amatuni Ts.A. et al. Nucl.Instr. and Meth. 203(1982) 179.

[7] Khazins D.M. et al. Nucl.Instr. and Meth. A300(1991) 281.

[8] Aseev A.A. et al. Proceedings of the 3-rd Workshop "Physics at UNK", Protvino, 1991, p.102.

[9] Demortier L. et al. Preprint FERMILAB-Pub-92/190, Batavia, 1992.

[10] Batalov A. et al. Preprint IHEP 92-102, Protvino, 1992.

[11] Barranco-Luque M. et al.Preprint BNL 31011, Brookhaven, 1982.

[12] Fanourakis G. Recent Results on High Pressure Gas Calorimetry, the 3-d Inter. Conf. on Calorimetry in High Energy Physics. September 29 - Oct. 2, 1992. Corpus Christi, Texas.

[13] Denisov S.P. et al. Preprint IHEP 92-98, Protvino, 1992. Denisov S.P. et al. Preprint IHEP 93-17, Protvino, 1993.

[14] Babintsev V.V. Preprint IHEP 92-20, Protvino, 1992. Babintsev V.V. Preprint IHEP 92-164, Protvino, 1992.

[15] Budagov Yu.A. et al. Forward Calorimetry for Tev-Colliders, Communication of the JINR E1-91-572, Dubna, 1991.

[16] Khazins D.M. et al. A high pressure gas ionization tube calorimeter for forward detectors. FERMILAB-PUB-92/393, submitted to NIM.

[17] Krasnokutsky R.N. et al. Fiz.Elem.Chastits i At.Yadra, 22(1), 1991.

[18] Krasnokutsky R.N. et al. Sov.J.Part.Nucl.,22(1), January-February 1991, p.125.

[19] Krasnokutsky R.N. et al. Preprint IHEP 91-48, Protvino, 1991. Krasnokutsky R.N. et al. Preprint IHEP 92-126, Protvino, 1992. Krasnokutsky R.N. et al. Preprint IHEP 92-139, Protvino, 1992.

[20] Fediakin N.N. et al. Nucl.Instr.and Meth.,A317(1992) 313.

[21] Chase R.L. et al. Transmission lines connection between detector and front-end electronics in liquid argon calorimetry. Preprint LAL (Orsay) 1992; submitted to NIM.

[22] Peisert A., F.Sauli F. CERN Preprint 84-08, Geneva, 1984.

[23] Dolgoshein B. et al. Nucl.Instr.and Meth. (to be published).

[24] Yamashita T. et al. Nucl.Instr.and Meth., A317(1992) 213.

Received September 23, 1993

В.Ф.Константинов и др.
Тесты модулей газового калориметра высокого давления.

Оригинал-макет подготовлен с помощью системы LaTeX.
Редактор А.А.Антипова. Корректор Е.Н.Горина.

Подписано к печати 23.09.1993 г. Формат 60 × 90/16.
Офсетная печать. Печ.л. 1,18. Уч.-изд.л. 1,41. Тираж 260. Заказ 936.
Индекс 3649. Цена 210 руб.

Институт физики высоких энергий, 142284, Протвино Московской обл.

210 руб. Индекс 3649

ПРЕПРИНТ 93-117, ИФВЭ, 1994